

An Approach to Real-Time Transient Stability Assessment and Control

Mania Pavella, Louis Wehenkel*, Arlan Bettio†, Damien Ernst
University of Liège, Sart-tilman B28, B-4000 Liège, Belgium

* Research Associate, F.N.R.S.

† On leave from University of Vale do Itajaí (UNIVALI), Brazil

Abstract. A unified approach to transient stability assessment is presented. It relies on a hybrid method, combining the equal-area criterion with a "generalized OMIB" which transforms a multimachine power system into a one-machine equivalent. The power system data may be provided by time-domain simulations or real-time measurements. Accordingly, the resulting approach is of the preventive or of the emergency type. The method is illustrated on realistic examples and validated via large-scale simulations performed on a variety of real-world power systems.

Keywords. Transient stability assessment (TSA); preventive TSA; real-time preventive TSA and control; real-time emergency control; hybrid methods; generalized one-machine equivalent.

1 A BRIEF HISTORICAL PERSPECTIVE

Transient stability studies started being developed around the first quarter of our century. One of the very first approaches was the equal-area criterion (EAC) [1, 2]. This criterion has important potentialities; but at that time it was restricted to a one-machine infinite bus (OMIB) system, where the machine and its connection to the infinite bus were modeled in a (over)simplified way.

Almost simultaneously, other approaches were also developed, such as, e.g., network analyzers and point-by-point methods of solving the swing equations [3]. The advent of computers encouraged large-scale computations of the swing equations. The interest of these "time-domain" methods is that they may handle any power system modeling and stability conditions and may provide, step-by-step, any details of the swing curves. But, on the other hand, they provide a "black-box" assessment: they are unable to appraise stability margins and to suggest control actions. Besides, at the early stage of their use, time-domain methods were too slow and hence incompatible with real-time requirements.

The so-called "direct methods", based on the Lyapunov direct criterion started being developed in the mid 60s; aiming to alleviate some of the above deficiencies. However, intensive research and promising preliminary results also revealed some inherent difficulties. Broadly, they are of two types, namely: (i) the construction of Lyapunov functions shows to be possible only with (over)simplified multimachine power system models; (ii) the stability domain is difficult to estimate rapidly and accurately (i.e. to circumvent the conservativeness of the Lyapunov theory which provides sufficient but not necessary conditions of stability) [4 to 6].

Automatic learning methods started being developed almost simultaneously with direct methods. Quite soon, however, it became clear that the computer facilities available at that moment were insufficient to meet their demanding needs. Thus, despite some thoughtful attempts, automatic learning has been in stand-by for about two decades.

To circumvent some of the direct methods' difficulties, OMIB equivalents were developed around the mid 80s: Rahimi and Schaffer proposed a "worst case" approach [7]; Xue et al. the so-called EEAC (for Extended EAC) [8]. These approaches rely on the observation that the loss of synchronism of a power system originates from the irrevocable separation of its machines into two groups; accordingly, they decompose the system machines into these groups, that finally reduce to an OMIB equivalent. This OMIB has important assets: it may use the EAC to get sufficient and necessary stability conditions and closed form expressions, easy to manipulate and compute. However, these attractive features are obtained under strong simplifying assumptions concerning both the power system model and the machines' behaviour during the transients. Nevertheless, the first practical results on real-world power systems were very promising; potential users started thus being interested in further developments, able to relax the method from the above simplifying assumptions (e.g., see [9]).

What is the state of the art in transient stability methods today ?

Paper presented at the 1997 IEEE PES Summer Meeting Panel Session on Transient Stability Limit Search, Berlin, Germany.

Time-domain methods. The tremendous progress in computer performances - and to a lesser extent in parallel processing - greatly contributed to bringing the methods close to real-time requirements; making them "faster than real time" is now within reach. One of two main weaknesses of time-domain methods has thus been removed. Yet, their "black-box" behaviour still remains.

Direct methods of the multimachine type. To get rid of modeling limitations, the general trend is to use "hybrid" approaches where multimachine time-domain trajectories provided by transient stability programs are used together with "pseudo-Lyapunov" functions. To overcome conservativeness, a bunch of skillful solutions has been proposed. These various improvements helped to reach one of their major objectives, viz., to provide stability margins [4 to 6].

Automatic learning approaches. After a latent period of about two decades, they started actively being developed around the mid eighties. Beginning with ANN approaches, they have gradually turned to machine learning methods, yielding decision trees, further complemented with k -NN methods. By now, a number of automatic learning methods, often hybridized are available (e.g., see [10]).

Direct methods of the "one-machine equivalent" type. During the last decade many variants have been developed, ranging from the simplest ones, based on the coherency and simplified modeling assumptions, up to more sophisticated, relying on "time-varying" or on "generalized" OMIBs described below.

The generalized OMIB concept is the basis of a hybrid method called SIME (for Single Machine Equivalent). Section 2 introduces this OMIB, while Section 3 derives general features of SIME. Section 4 describes the "preventive SIME" and Section 5 the "emergency SIME". Section 6 reports on simulation results.

2 OMIB TYPES AND THEIR DYNAMICS

(This section is transcribed from Ref. [11].)

The methods relying on an OMIB equivalent call upon the observation that the loss of synchronism of a multimachine power system originates from the irrevocable separation of its machines into two groups, which may be successively replaced by a two-machine and an OMIB equivalent. Thus, an OMIB may be viewed as a transformation of the multidimensional multimachine dynamic equations into a single dynamic equation. This latter takes on various forms, depending upon the power system modeling and the assumed behaviour of the machines within each group. Three types of OMIBs may be distinguished: "time-invariant", "time-varying" and "generalized" ones. They are briefly described below.

2.1 Time-invariant OMIB

A time-invariant OMIB is obtained under the following two assumptions: (i) simplified power system modeling; (ii) coherency of the machines within each one of the two groups, so as to "freeze" their relative motion in the during- and the post-fault periods.

The dynamic equations of a multimachine system may therefore be transformed into an equivalent OMIB equation of the form [7,8]

$$M\ddot{\delta} = P_a = P_m - P_e = P - P_{\max} \sin(\delta - \nu) \quad (1)$$

where M , P , P_{\max} and ν take on constant values (different in the during-fault and the post-fault configurations); hence the

name "time-invariant" OMIB. Note that eq. (1) is similar to that of the simple one-machine infinite bus system. It describes the typical sinusoidal variation on the $P_a - \delta$ plane, to which the well-known EAC criterion can be applied.

The combined use of this OMIB with EAC gave rise to the BEAC (e.g., see [8]).

2.2 Time-varying and generalized OMIBs

If, while keeping the simplified power system model we relax its machines from the coherency assumption we get "time-varying" OMIBs: P , P_{\max} , ν are not anymore constant, and the dynamics in eq. (1) becomes piece-wise sinusoidal. Such time-varying OMIBs were for instance used in the GEAC (for Generalized EAC) [12] and in the DEEAC (for Dynamic BEAC), e.g., see [6].

If, in addition, we consider detailed power system models, we come up with what we call the "generalized" OMIB. The dynamics of this OMIB is still expressed by

$$M\ddot{\delta} = M\dot{\omega} = M\gamma = P_a = P_m - P_e; \quad (2)$$

but, here, the $P_a - \delta$ variation is no longer sinusoidal (see Figs 1 commented below), nevertheless, the principle of the EAC is still applicable (see § 3.3).

In eq. (2), the OMIB parameters (δ , ω , P_m , P_e) are obtained via a suitable transformation of the multimachine parameters; these latter may be obtained via time-domain simulations or real-time measurements. By combining the advantages of the multimachine time-varying data with those of the EAC, the generalized OMIB provides very fast and rich information about transient stability.

Remark

The generalized OMIB concept is on the basis of various recent approaches, for example the "mixed" BEAC [6], the HEAC (for hybrid BEAC), the IBEAC (for Integrated BEAC) [13], the FASTEST [14], the SIME [15].¹ These approaches differ in many respects, e.g., in the way of identifying the mode of machines' separation, of refreshing the OMIB parameters, of computing the stable and unstable margins, of assessing stability limits, of filtering contingencies. Below we elaborate on the SIME approach.

3 THE GENERALIZED OMIB WITHIN SIME

The main properties of the generalized OMIB enumerated in [11] are expounded here in the context of the SIME method. These properties will then be used to devise the preventive and the emergency SIME.

The description is illustrated on an example of the preventive SIME applied to a real-world stability case of the EDF EHV power system [15]. The considered contingency is a three-phase short-circuit, cleared at two different times, one smaller and one larger than the critical clearing time (see Figs 1). The system is represented with detailed load and machine modeling, comprising in particular AVR's and fast valving. In Figs 1, the

¹A detailed account of the many variants is beyond our scope; we therefore mention them without systematically referring to the publications where they (first) appear.

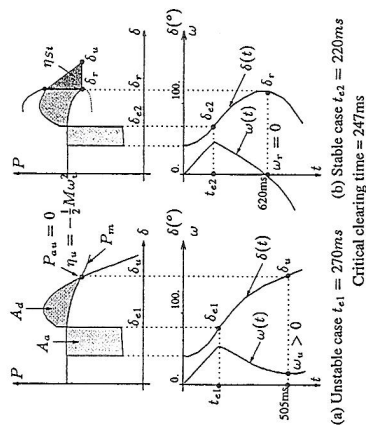


Figure 1. Illustrating the EAC and OMIB trajectory properties. Adapted from [15]

decline of P_m is due to the influence of fast valving. Observe also that the post-fault P_e vs δ curve is not sinusoidal - but still resembles one.

3.1 Critical machines and OMIB identification

On an unstable time-domain trajectory, the critical machines are those which cause the system loss of synchronism. Accordingly, to identify them, SIME observes the post-fault swing curves of the system machines computed via a time-domain program. At each step, it sorts the machines in decreasing order of their rotor angles, identifies the largest angular deviation (largest "gap") between any two adjacent machines thus sorted, and considers the candidate critical cluster of concern to be the one which is "above this largest gap". The corresponding candidate OMIB's trajectory is computed as explained in § 3.2. The procedure is carried out until the candidate OMIB reaches its unstable angle δ_u (defined in § 3.3); it is then declared to be the critical OMIB.

Let us insist that a critical OMIB is defined on an unstable case only. By continuation, we consider it to be still valid on a borderline stable case.

Figures 2 illustrate the critical machines identification procedure.

3.2 Critical OMIB parameters

Let C denote the group of critical (or advanced) machines and N that of the non-critical (or backward) machines. The corresponding critical OMIB parameters δ , ω , M , P_m , P_e are readily computed as follows.

(i) Transform the two clusters into two equivalent machines, using their corresponding partial center of angle. E.g., for cluster C this results in

$$\delta_c(t) \triangleq M_C^{-1} \sum_{k \in C} M_k \delta_k(t) \text{ with } M_C = \sum_{k \in C} M_k. \quad (3)$$

Similar expressions hold for cluster N , and yield the angle δ_N .

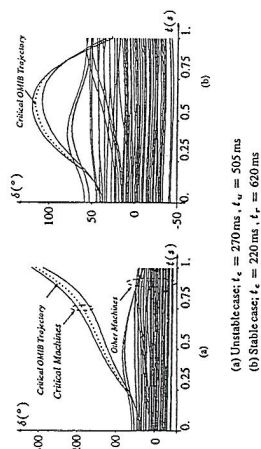


Figure 2. Illustrating critical machines and OMIB identification. Adapted from [15]

(ii) Reduce this two-machine system into an equivalent OMIB system whose rotor angle is defined by

$$\delta(t) \triangleq \delta_C(t) - \delta_N(t) \quad (4)$$

and whose rotor speed, ω , is defined in a similar way.

(iii) Define the equivalent OMIB mechanical power by

$$P_m(t) = M \left(M_C^{-1} \sum_{k \in C} P_{mk}(t) - M_N^{-1} \sum_{j \in N} P_{mj}(t) \right) \quad (5)$$

where $M = M_C M_N / (M_C + M_N)$ is the equivalent OMIB inertia coefficient. The OMIB electrical power P_e takes on a similar expression. Note that all individual machines' mechanical (P_{mk} 's) and electrical (P_{mj} 's) powers are considered to be free from any simplifying assumption, and so are the derived OMIB powers $P_m(t)$, $P_e(t)$. Note also that the above parameters $\delta(t)$, $\omega(t)$, $P_m(t)$, ... are computed at each time step of the time-domain program.

Figures 2 portray the OMIB trajectories plotted from the multimachine system swing curves.

3.3 Calculation of stability margins

The equation of motion of the OMIB equivalent

$$M\ddot{\delta} = M\dot{\omega} = P_m - P_e = P_a \quad (6)$$

where P_a is the accelerating power, expresses in particular its power-angle dynamics.

A direct transient stability assessment of the above dynamic system is provided by the well-known equal-area criterion via the notion of stability margin:

$$\eta = A_{dec} - A_{acc}. \quad (7)$$

This criterion states that: for a given stability scenario the OMIB system is unstable (resp. stable) if $\eta < 0$ (resp. $\eta > 0$). The borderline case, $\eta = 0$, provides the limit (in stability condition, in terms of critical clearing time or power limit).

Equations (6), (7) yield the following margin expressions:

- unstable margin:
$$\eta_u = -\frac{1}{2} M \omega_u^2 \quad (8)$$

- stable margin :

$$\eta_{st} = \int_{\delta_r}^{\delta_u} |P_a| d\delta \quad (9)$$

In these expressions,

- suffix a (for unstable) refers to the angle δ_u and time t_u where
- suffix r (for return) refers to the angle δ_r and time t_r where δ starts decreasing and ω vanishes.

$$P_a = 0, \quad \dot{P}_a > 0; \quad (10)$$

Figures 1 illustrate the equal-area criterion in the unstable and stable cases portrayed in Figs 2.

Note that eq. (9) must be approximated [15, 16]. In particular, Ref. [16] uses the extrapolation procedure described below.

3.4 Extrapolation/prediction of the curve $P_a - \delta$

Even if the $P_a - \delta$ variation differs from a sinusoid, it still keeps similar shape. This suggests various ways of "projecting" (i.e. either extrapolating or predicting) a restricted part ahead of the existing curve.

For example, Ref. [16] uses the expression

$$P_a(\delta) \approx a\delta^2 + b\delta + c \quad (11)$$

and solves for a, b, c , based on P_a values taken at three successive times on the known part of the $P_a - \delta$ curve.

Note that SIMB owes this extrapolation/prediction possibility to the OMBB representation; indeed, the same type of approximation used separately for each one of the multimachines' $P_{ai} - \delta_i$ curves would lead to an accumulation of errors and overly erroneous assessment.

The extrapolation property is used to compute stable margins; the prediction property is at the heart of the emergency SIME.

3.5 Compensation schemes

Another important property of the OMBB representation is its ability to answer the following two questions relating to an unstable situation : (i) "how much" unstable the system is ? (ii) how to compensate the instability so as to recover stability ?

Answering question (i) amounts to computing the negative margin according to eq. (8). To answer question (ii), observe that the system stability may be reinforced by decreasing A_d and/or increasing A_f (see Fig. 1a); or, stated otherwise, by decreasing P_m and/or increasing the post-fault P_e , or by decreasing the clearing time.

Such compensation schemes are proposed below in Section 4.

4 PREVENTIVE SIME

The preventive SIME uses a time-domain transient stability program to compute at each time step the generalized OMBB parameters for real-time transient stability analysis and control.

Analysis deals with contingency severity assessment; it generally comprises two steps : contingency screening (to identify

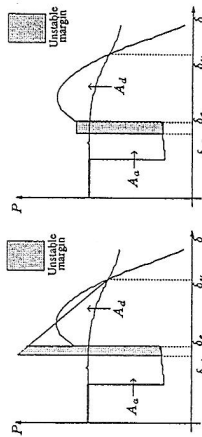


Figure 4. Two compensation schemes for contingency screening [16]
 $t_e = 270$ ms ; $t_{e1} = 237$ ms ; $t_{e2} = 212$ ms, CCT = 247 ms

the stability case of Fig. 1a : the shaded area is designed so as to compensate for the unstable margin value (schematically represented by the dark rectangle) by decreasing the accelerating and increasing the decelerating areas. Accordingly, the compensation scheme of Fig. 4a (respectively 4b) yields the approximate critical clearing angle δ_{c1} (resp. δ_{c2}), from which the corresponding assessment of t_{e1} (t_{e2}) is readily obtained.

While this - admittedly promising "compensation filter" needs further elaboration, the "extrapolation filter" has extensively been validated and shown to be very efficient (see Section 6).

4.2.2. Sequence of filters

Using a sequence of filters with increasing modeling details may provide substantial computing gains, since a good deal of the contingencies are likely to be discarded by SIME with simplified modeling which is computationally faster than SIME with detailed modeling.

Note, however that it may happen - though quite seldom - that stability limits with simplified modeling are larger - instead of smaller than with detailed modeling; but, whenever it arises, this "inversion" is marginal. Nevertheless, this leads to choosing large enough threshold values to avoid missing potentially harmful contingencies.

Note also that simplified modeling may not be appropriate for some power systems.

Finally, observe that screening contingencies in terms of CCT's is much faster than in terms of power limits.

Taking advantage of the above observations yields quite a large variety of possibilities; when properly used, they provide very important computing gains, and make contingency screening and assessment compatible with real-time preventive monitoring.

4.3 Stability limits computation

The accurate assessment of a stability limit (critical clearing time or power limit) simply amounts to refining the stability assessment provided by the filtering procedure, by using few additional margin values. In the example of Fig. 3, using a power level lower than 2712 MW is likely to provide stable conditions and hence a positive margin; using this latter together with the

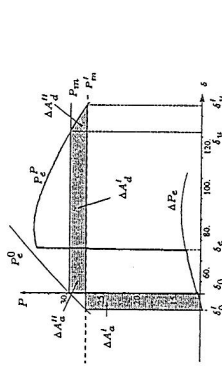


Figure 5. A compensation scheme for assessing generation power limits

closest negative one provides a refined power limit assessment. (In the figure, the resulting value of 2654 MW is close to that provided by a pure time-domain program (2670 MW) [15].)

Note that the possibility of "guiding" the procedure thanks to margin values allows the method to converge much more efficiently to the solution than dichotomy (often used in time-domain searches).

4.4 Suggestions to control

An unstable case raises the two questions of § 3.5. : Question (i) ("how much unstable the case is ?") calls upon margin computations; question (ii) ("how to cancel out the presumably negative margin ?") calls upon compensation schemes which in turn rely on the identification of the critical machines.

Such a compensation scheme consists of lowering the OMBB mechanical power P_m . Figure 5 sketches a "brute force" approximation where the variations $\Delta A_d^u, \Delta A_d^s, \Delta A_f^u, \Delta A_f^s$ result from the decrease of P_m under the assumption that this latter does not affect the curve P_e^0 . Assuming further that the effect of ΔA_d^u is approximately compensated by the effect of ΔA_f^u and ΔA_f^s yields

$$\Delta P_m = P_m - P_m' \approx \frac{M\omega_u^2}{2(\delta_u - \delta_c)}$$

Now, according to eq. (5), decreasing the OMBB mechanical power P_m amounts to decreasing the power of critical machines ($P_{m,c}$) and/or increasing the power of non critical ones ($P_{m,n}$). Obviously, this relies on the correct identification of the critical machines.

A broad perspective of compensation means is given in [18], while [19] elaborates on the real-time approach outlined below.

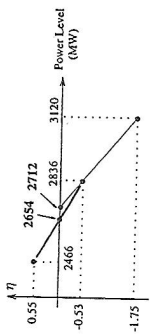
5 EMERGENCY SIME

5.1 Introduction

The emergency SIME relies on the same concepts as the preventive SIME; but it differs in the way of exploiting them.

A first main difference is that in the emergency context the OMBB parameters (δ, ω, P_a) are computed from real-time measurements acquired at the power plants. Another important difference is that, here, the concern is the stability assessment

Figure 3. Search of stability limits by extra(inter)-polating decreasing margin values. Taken from [15]



and discard the harmless contingencies), and stability limit computation (to scrutinize the potentially harmful ones). Both steps rely on stability margins, since a stability limit corresponds to zero-margin conditions.

Note that the computation of a margin requires very short time-domain simulations; indeed, these simulations are stopped as soon as the unstable or stable conditions are met (for example, in Figs 1 and 2 the times corresponding to reaching δ_u and δ_r are respectively of 505 and 620 ms).

4.1 Stability margins computation

An unstable margin is computed precisely using eq. (8). But a stable margin expressed by (9) may be computed only approximately, since the $P_a(\delta)$ curve does not actually exist in the interval (δ_r, δ_u) (the OMBB angle of a stable simulation reaches a maximum value δ_r , then starts decreasing). A convenient approximation consists of extrapolating the $P_a - \delta$ curve, as suggested in § 3.4. Note that the closer the stable scenario to the borderline case $\eta = 0$, the better the approximation.

4.2 Contingency screening

The purpose of screening (generally a large list of) contingencies is to discard the harmless ones (generally the major part of the list), and select to further scrutinize the potentially harmful contingencies. It is therefore possible to speed up contingency screening by using approximations along three lines : (i) accuracy range; (ii) modeling sophistication; (iii) type of stability limit sought.

4.2.1 Contingency screening schemes

Two such schemes are proposed below.

The extra(inter)-polation scheme uses two margin values computed for two (relatively close) stability conditions that extra- (inter-)polates to get an approximate limit value; its comparison with the preassigned threshold value allows discarding or keeping the contingency, as appropriate. Figure 3 suggests that the linear extrapolation of two margin values corresponding to two unstable power levels (of 3,120 and 2,836 MW) yields an approximate power limit of 2,712 MW (to be compared with the accurate power limit of 2,654 MW, see § 4.3).

The compensation scheme relies on a sole unstable margin and consists of assessing "how much" the stability conditions should be changed in order to cancel out this margin. Two such compensation schemes furnishing approximate assessment of critical clearing times were proposed by Y. Zhang [17]. The principle is schematically described in Figs 4 corresponding to

on the basis of measurements corresponding to the system post-fault configuration, i.e. after a disturbance inception and its elimination by the protective devices. Hence, the specific tasks assigned to the emergency SIME are [19]: after reaching the post-fault configuration, (i) assess the system stability; (ii) appraise the severity of instability, whenever detected; (iii) identify the corrective action to be taken (e.g., how much generation to shed and (out of) which generator(s)).

Note that in this emergency context, the overall procedure must be faster than the "time to instability", so as to prevent loss of synchronism. Observing that the earlier the control action is triggered the more effective it is, and since the time for the system to go unstable can be shorter than 1 second, the target is to trigger the control action within at most 400 ms after fault clearing.

Remark. The type of emergency control provided by the emergency SIME is called "during transients" to emphasize that the method relies on real-time measurements only, which contain all information relevant to transient stability (e.g., type and location of the actual contingency, and even the very system post-fault topology). On the basis of these measurements, the method appraises system's stability and designs/decides on-line control actions.

5.2 Emergency-specific analysis tasks

5.2.1 Prediction of the $P_a - \delta$ curve

The general prediction scheme of § 3.4 is still applicable. But, here, the mode of machines' separation is not known, since the prediction should be accomplished long enough before reaching the (un)stable conditions. Hence, the first task consists of predicting the critical OMIB. This leads to the following sequence of tasks.

- (i) At a time t_i short after the disturbance clearance, ($t_i \geq t_e + 2\Delta t$), use Taylor series to predict the individual machine angles at some time ahead (e.g. 100ms). Sort the machines in decreasing order of these angles and consider as candidate critical machines those advanced machines which are above the largest gap.
- (ii) Construct the corresponding OMIB, determine its parameters ($\delta, \omega, \gamma, P_c$) from the corresponding parameters of the individual power plants at times $t_i - 2\Delta t$, $t_i - \Delta t$, t_i , and approximate the $P_a - \delta$ curve by solving the expression (11) for a, b, c at these times.
- (iii) Solve eq. (11) to find $\delta_c > \delta(t_i)$ which meets conditions (10).
- (iv) Compute the decelerating area, A_d (e.g., see Fig. 6 commented below).
- (v) If η is found to be negative or close to zero, declare the system to be unstable and determine control actions.
- (vi) Acquire a new set of measurements and continue monitoring the system.

5.2.2 Comments

- 1.- Computationally, the above strategy is extraordinarily unexpensive and fast; indeed, at each time sample, it merely requires (a) the solution of the individual Taylor series and

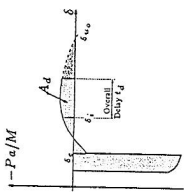


Figure 6. Principle of emergency control

OMIB identification; (b) computation of the OMIB parameters (see eqs (3) to (5), and of the P_a curve (11)); (c) computation of the margin (8). Obviously, all these computations require only fractions of ms.

2.- The candidate critical machines identified in step (i) are not necessarily the machines composing the actual critical cluster, i.e. the group of machines which would be responsible of loss of synchronism. Nevertheless, taking control actions on these machines will anyhow reduce the system kinetic energy, i.e. will stabilize it, even if not in an optimal way.

3.- An interesting information is the "time to instability", i.e. the time for the system to lose synchronism if corrective actions are not taken. In the OMIB representation this corresponds to a time slightly larger than t_u , and may be computed for example via a Taylor series expansion of $\delta(t)$ about $\delta_c(t_i)$.

5.3 Emergency control actions

For negative margins, the question of concern is: which corrective actions should be taken to satisfactorily stabilize the system? In practice, two main types of control actions may be thought of to increase the OMIB decelerating power: (i) reduce the mechanical power (e.g. fast-valving); this is rather easy to evaluate in the time frame considered in a real-time emergency context; (ii) increase the electrical power (e.g., braking resistors, DC links, and thyristor controlled series compensators), accurate evaluation of their effect may be more difficult, in particular because of the coupling of network equations.

The control scheme proposed in [19] reduces the mechanical power by shedding generation. The generators to be shed are chosen among those belonging to the critical cluster, as identified in § 5.2. On the other hand, the amount of generation to be shed so as to increase the decelerating area A_d depends on the size of the (negative) margin (see Fig. 6, drawn on the plane $(-P_a, \delta)$). Subsequently, i.e. after the corresponding control order has been sent to the generation plant, it is important to continue refining and if necessary adjusting the assessment using new real-time measurements. Note that, because of the transmission delays, the incoming new measurements still correspond for a while to the uncontrolled system; hence, the changes introduced by the control should be anticipated; Ref. [19] proposes such a prediction scheme.

Remarks

- 1.- An essential asset of this during-transients approach is its adaptability to any kind of operating and fault conditions. Moreover, being free from off-line (or preventive mode) tuning,

it is intrinsically robust with respect to modeling errors, and able to cope with unforeseen events.

2.- Another method's asset is its high computational efficiency. This makes it able to work in a closed loop fashion, i.e. to be robust with respect to its own prediction errors. The method could thus be applied to a large variety of control means.

Admittedly, the proposed approach is in its infancy, and important developments are still needed. Below we skim over some open methodological questions, while skipping hardware aspects.

(i) Need for developing proper control actions of various types in addition to the generation shedding scheme [19].

(ii) Need for development of approximate local procedures which would approximate data coming from irrelevant machines and/or parts of the network far away from the contingency location.

(iii) Control actions deemed "too slow" and hence unable to be used alone should be complemented with preventive actions; these latter could however be taken quite parcimoniously as long as emergency control actions are able to complement them in real-time if necessary (see in § 6.2.2 comments relative to a real-world example.)

The above discussion emphasizes that specific power systems and practices call for different solutions; the combinatorial further increases when considering different "optimality" criteria (economy vs security, availability and cost of hardware resources, etc). It is therefore desirable to design a range of possible actions, keeping in mind that, generally, the more accurate a control action and the more demanding, for example, centralized control would be more accurate than local, but more demanding in terms of communication facilities.

6 REAL-WORLD SIMULATIONS

The mechanisms of SIME are illustrated and validation tests are described. The illustrations concern both the preventive and the emergency SIME (§§ 6.1 and 6.2 respectively); the validation tests concern the preventive SIME (§ 6.3).

6.1 Illustrating the preventive SIME

Two types of illustrations are considered; the one concerns computation of stability limits (power limits and critical clearing times), the other contingency screening.

6.1.1 Stability limits computation

First illustration: power limit assessment. This example is borrowed from Ref. [20] which deals with power limits of the Hydro-Québec (H-Q) EHV power system. Hence, SIME is coupled with the H-Q ST600 program and the standard (detailed) model used at Hydro-Québec for operation planning studies [21]. The ST600 program is also used as the reference for comparisons.

The base case corresponds to a peak load situation (35,000 MW load + 2,000 MW losses). The model comprises 514 buses, 682 branches and 94 generators.

Table 1 describes the details of the computation of the power generation limit in the Churchill Falls (CF) plant with respect to

Table 1: Power generation limit assessment of CF
At $t=0.000$ s, 3 ϕ SC on a line
At $t=0.083$ s, trip of this line
At $t=0.250$ s, shedding of 2 units in CF (2×506 MW)

1	2	3	4
$P(k)$ (MW)	Nr of crit. m/s	$P(k-1)$ $P(k)$	$P(L(k))$ (MW)
4560	23(1st swing)	—	—
4560/1.1 = 4145	23(1st swing)	-1.42	3984
3984 - 100 = 3884	23(3rd swing)	-1.42	—
3884/1.1 = 3699	—	-1.29	3774

P and P_L concern the total post-fault generation in the CF plant
 P_L provided by the pure time-domain program: 3760 MW

a typical contingency, applied to a weakened pre-fault situation.

The successive rows in Table 1 correspond to decreasing post-fault generation levels in the CF plant P at successive iterations of the SIME procedure. The information provided in the columns is: (1) the power level at step k ; (2) the number of relevant machines of an unstable simulation; (3) the margins of the relevant OMIB for power levels at steps $k-1$ and k ; (4) the stability limit as extrapolated or interpolated; the value in bold indicates the limit power found by SIME.

The procedure starts with an initial level of 4,560 MW corresponding to the base case: it is found to be first-swing unstable with a negative margin of $\eta = -1.42$; there are 23 critical machines losing synchronism.

The next step is obtained by reducing the amount of generation by about 10%. The critical cluster is the same as previously. The simulation yields a slightly negative margin of -0.41 . This, together with the margin of -1.42 yields by extrapolation the limit $P_L = 3,984$ MW. The difference between this and the last simulated power level of 4,145 MW is of 161 MW. To get a better estimate of P_L while at the same time exploring about the existence of multi-swing phenomena, a new power level lower to P_L by 100 MW is chosen. The obtained results are reported in the lower part of Table 1: for $P = 3,884$ MW the same as above 23-machine critical cluster experiences a 3rd swing instability, whereas for the next power level of 3,699 MW the multimachine system is stable throughout the 15-second integration period. The power limit is obtained by interpolation and amounts to 3,774 MW, which is in agreement with the pure time-domain assessment of the ST600 program (3,760 MW).

Second example: critical clearing time assessment. This example is taken from a CIGRE exercise using the IEEE 50-machine system, where part of the machines are equipped with AVRs. The concern is the critical clearing time (CCT) of a 3-phase short-circuit. Here, SIME is coupled with EUROSTAG [22].

Table 2 summarizes the simulation results obtained with a maximum integration period of 5 s. They call for the following observations. The first clearing time is automatically chosen by stopping the during-fault simulations as soon as a maximum deviation between any two machines reaches 180° . Here, this clearing

²The corresponding pre-fault level is obtained by adding the 1012 MW of the generators shed.

Table 2 : Critical clearing time assessment

1	2	3	4
$t_c(k)$	Nr of rel. m.	η	$t_c(k)$
250	29	—	(ms)
250/1.1 = 227	—	-0.22	—
		6.20	248

CCT provided by the pure time-domain program : 248 ms

ing time, $t_c = 250$ ms. In the second iteration ($t_c = 227$ ms), the system becomes stable, the CCT is therefore computed by interpolation and found to be of 248 ms; this coincides with the reference value provided by EUROSTAG run alone.

Discussion. The above two examples are quite typical of the way SIME assesses stability. In particular, the examples suggest that

- (i) in general, 2 to 3 unstable simulations are enough to appraise the stability limit sought, using increasing (i.e. decreasing moduli of negative) margin values
- (ii) to explore stable simulation is necessary whenever one wants to whole possible existence of multi-swing phenomena and appraise the corresponding limits.

The method's accuracy depends on how closely it approaches the zero-margin conditions "from the right", i.e. on the number of unstable simulations. Computationally, this is much less expensive than a dichotomical approach which, in particular, requires many stable simulations.

The above assessment is corroborated by a large number of simulations.

6.1.2 Contingency screening

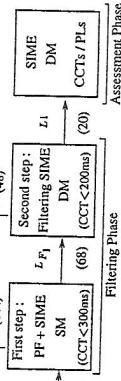


Figure 7. A sequence of SIME filters and resulting contingency selection (Taken from [23])

Figure 7 proposes a contingency screening scheme using two filters in a row with increasing modeling refinement, followed by an accurate assessment with detailed model. In this figure, PF denotes a prefiler, consisting of special purpose time-domain program with very large steps; SM (resp. DM) stands for simplified model (resp. detailed model).

The figure is borrowed from a case study run on the South-Southeast Brazilian power system (1,180 buses, 1,962 branches, 56 machines) [23]. It shows that out of the 712 contingencies screened by the two filtering steps, only 20 are eventually selected as being potentially "harmful".

6.2 Illustrating the emergency SIME

The following real-world example is borrowed from Ref. [19] which considers a generation shedding scheme for

off-line, so that the only real-time action is to recognize the fault condition and trip the generators.

While being slightly slower (350 ms instead of 250 ms), the advantage of the during-transients strategy illustrated above is its intrinsic capability to adapt the number of generators to shed according to operating and fault conditions. Furthermore, being based on (real-time) measurements rather than numerical simulations and using closed loop operation provides inherent robustness to modeling and measurements errors.

2.- It is also interesting to notice that it is actually possible to stabilize the system by shedding only one generator, provided that the shedding is triggered before $t = 257$ ms. Hence, with the hardware available at Hydro-Québec, a cautious (i.e. precautionous) action could be taken at 250 ms, given that emergency control could complement it in real-time if necessary.

The above discussion suggests that the combination of preventive and emergency control schemes may yield interesting solutions.

6.3 Validation tests

The preventive SIME was validated through extensive simulations performed on various test systems and the following real-world power systems :

- IBBE 50-machine system (coupled with EUROSTAG)
- EDF EHV system (many variants; coupled with EUROSTAG)
- Hydro-Québec EHV system (coupled with ST600)
- South-Southeast Brazilian system (coupled with ST600).

The IBBE 50-machine system was simulated with standard simplified modeling and partly detailed one. Simulations with the EDF and the South-Southeast Brazilian system have been considering both the standard simplified model and their respective full modeling. The Hydro-Québec system was run with its full model.

The simulations concern search of both critical clearing times and power limits. All in all, many thousands of stability cases were simulated. The results were found to be consistently accurate.

6.4 Preventive SIME vs TD methods

Figure 8 points out main similarities and differences of SIME with time-domain (TD) programs.

7 CONCLUSION

This paper has reported on an emerging type of methods : a hybrid time-domain—direct method, relying on an single-machine equivalent.

The purpose has been to provide a comprehensive, unified approach to preventive and emergency real-time transient stability assessment and control. The focus has been on conceptual aspects rather than implementation details.

Another aim of the paper has been to emphasize the method rich potentialities, combining those of time-domain methods together with many others proper to the generalized one-machine

The preventive SIME is

- as general as the time-domain (TD) program with respect to
 - power system modeling
 - stability scenarios
 - type of stability limits sought (critical clearing times or power limits)
 - type of (in)stability (first- or multi-swing) and mode (plant or interarea)
- as accurate as the TD program
- much faster than the TD program
- much more informative than the TD program, since, in addition to the information provided by TD programs, SIME furnishes
 - stability margins
 - unambiguous identification of the relevant machines.

In short,

- SIME combines the advantages of TD and of direct methods, while evading their difficulties
- it can advantageously replace TD programs for planning and operation planning
- it makes feasible real-time transient stability monitoring and control.

Figure 8. Preventive SIME vs corresponding TD programs

equivalent. These additional potentialities are able to provide effective tools for real-time transient stability assessment and control which are sorely needed for the secure monitoring of power systems.

8 REFERENCES

- [1] Dahl O.G.C. (1938) *Electric Power Circuits. Vol. II: Power System Stability.* McGraw-Hill, Inc., New York.
- [2] Kimbark E.W. (1948) *Power System Stability.* Vol. I : *Elements of Stability Calculations.* John Wiley and Sons, Inc., New York.
- [3] Park R.H. and E.H. Bancker (1929) System stability as a design problem. *AIEE Trans.* 48 : 170-194.
- [4] Pai M.A. (1989) *Energy Function Analysis for Power System Stability.* Kluwer Academic Publishers.
- [5] Fouad A.A. and V. Vittal (1992) *Power System Transient Stability Analysis Using the Transient Energy Function Method.* Prentice-Hall Inc., Englewood Cliffs, N.J.
- [6] Pavella M. and P.G. Murthy (1994) *Transient Stability of Power Systems. Theory and Practice.* John Wiley & Sons, Chichester, England.
- [7] A. Rahimi and G. Schaeffer (1987) Power system transient stability indexes for on-line analysis of 'worst case' dynamic contingencies. *IEEE Trans.* PWRS-2 : 660-668.
- [8] Xue Y., Th. Van Cutsem and M. Ribbens-Pavella (1988) A simple direct method for fast transient stability assessment of large power systems. *IEEE Trans.* PWRS-3 : 400-412.

Table 3 : Successive predictions. Taken from [19]

t_i ms	η	δ_{sc}	δ_{sc}	X %
≤ 209	≥ 0	67.9	109.0	96
217	-0.765	70.9	106.4	92
233	-1.400	70.6	104.9	89
250	-1.700	70.6	104.9	89

1 generator shed $\rightarrow \Delta X = -10\%$

the Hydro-Québec system. For want of real-time measurements, the results are obtained via simulations with detailed system modeling carried out with the ST600 transient stability software of Hydro-Québec [21].

6.2.1 Description

The pre-fault topology considers one line out of operation and 10 machines in operation in the Churchill Falls (CF) power plant producing 5070 MW. At $t = 0$ a three-phase short-circuit is applied on a line and the system is supposed to enter the post-fault configuration at time $t_c = 83$ ms after the line is tripped. Real-time measurements are collected and predictions are started at this time instant at an observation rate of one sample per cycle.

Table 3 shows the predictions made at successive steps t_i 's. In this simulation it is supposed that the overall delay for the generation shedding is of six cycles (100ms, comprising the measurement, computation and triggering delays). As can be seen from the table, for $83 \text{ ms} < t_i \leq 209 \text{ ms}$ the prediction is that the system will be stable $X \geq 1$; but as soon as time reaches $t_i = 217$ ms, instability is predicted and the critical machines are found to be those of the CF power plant. It is therefore decided that one machine out of the 10 will be tripped, since this is sufficient to reach $X = 96\%$. Taking into account the overall delay of $t_d = 100$ ms the shedding will actually take place at time $t = 317$ ms.

The third row of Table 3 corresponds to the next observation step $t_i = 233$ ms. In order to check whether the previously triggered control action is sufficient, the value of X is recomputed on the basis of the incoming measurements. The result is that X should be smaller than 92% for stable operation (supposing that the control action is applied at time $t = 317$ ms). Thus, although the estimation at the previous step was quite optimistic, no additional control action is decided yet.

At the next observation step ($t_i = 250$ ms), however, a similar reasoning tells that another machine should actually be tripped. Taking into account again the delay we note that this action will take place only at time $t = 350$ ms.

Similar computations are made at subsequent time steps ($t_i > 250$ ms) in order to check whether these two successively triggered control actions will indeed stabilize the system. The answer is Yes, as is confirmed by the fact that the controlled system reaches a maximum angle and then swings back.

6.2.2 Comments

1.- It is interesting to mention that the generation shedding device implemented at Hydro-Québec would actually have triggered the shedding of two generators at $t = 250$ ms. Its higher speed is possible because it is based on a relay arming strategy in the preventive mode, based on power flow limits computed